Geophys. J. Int. (2014) **196,** 671–680
Advance Access publication 2013 November 13
doi: 10.1093/gji/ggt427

Constraining fault friction by re-examining earthquake nodal plane dips

Timothy A. Middleton* and Alex Copley
COMET+, Bullard Labs, Department of Earth Sciences, University of Cambridge, Cambridge, UK. E-mail: tim.middleton@earth.ox.ac.uk

Accepted 2013 October 10. Received 2013 August 22; in original form 2013 April 17

SUMMARY

We have assembled a catalogue of well-constrained focal mechanisms for earthquakes that occurred on continental dip-slip faults that have experienced only small displacements during their current phase of activity. Nodal planes for both reverse- and normal-faulting events are seen to vary between ∼30° and ∼60°, and are concentrated towards the centre of this range. The observed distributions suggest the reactivation of structures with a low coefficient of friction (less than ∼0.3, and possibly as low as ≤0.1). We propose that this low coefficient of friction corresponds to the presence of weak materials in pre-existing fault zones.

Key words: Friction; Fault zone rheology; Rheology and friction of fault zones; Continental neotectonics; Dynamics and mechanics of faulting.

1 INTRODUCTION

The frictional properties of active faults remain a major unsolved problem within the Earth Sciences. Early lab experiments suggested that the coefficient of friction (μ defined as the ratio of shear stress to normal stress at failure) is 0.85 at low confining pressures (<∼200 MPa) and 0.6 above this (Byerlee 1978). However, two factors prevent the simple application of this 'Byerlees Law' to the Earth. The first is that some materials that commonly form fault rocks, such as clay minerals and the deformed remains of the rocks bounding active fault zones, have experimentally derived coefficients of friction that are considerably lower than predicted by Byerlees Law (e.g. Byerlee 1978; Saffer *et al.* 2001; Brown *et al.* 2003; Collettini *et al.* 2009; Lockner *et al.* 2011). Secondly, the pore-fluid pressure at the depths where large earthquakes nucleate is unknown. Pore-fluids at high pressure reduce the effective normal stress acting across fault zones so, for a given coefficient of friction, failure can occur at lower shear stresses if the pore-fluid pressure is higher. Some geophysical arguments have suggested that the effective coefficient of friction on active faults may actually be much lower than 0.6, possibly as low as ∼0.1 (e.g. Lachenbruch & Sass 1980; Zoback *et al.* 1987; Lamb 2006; Herman *et al.* 2010; Copley *et al.* 2011). In contrast, a number of borehole measurements have indicated that the strength of the crust is limited by critically stressed faults with hydrostatic pore-fluid pressures and coefficients of friction in the range 0.6–1.0 (e.g. Zoback & Healy 1992; Brudy *et al.* 1997). However, some boreholes drilled through major active faults (e.g. Lockner *et al.* 2011), and field studies of exhumed faults (e.g. Collettini 2011, and references therein) have encountered low-friction fault rocks (e.g. $\mu < 0.4$). In view of this uncertainty regarding fault friction, this paper seeks to provide additional constraints on the mechanical properties of active faults, and so increase our understanding of the stress-state and rheology of the lithosphere.

One method that has previously been used to try and constrain the frictional properties of active faults is the analysis of the dip range over which continental dip-slip earthquakes occur (Jackson & White 1989; Thatcher & Hill 1991; Sibson & Xie 1998; Collettini & Sibson 2001). This paper takes a similar approach, but re-examines the frictional properties of faults by analysing a specific subset of an expanded catalogue of well-constrained earthquake focal mechanisms.

2 CONTINENTAL EARTHQUAKE FAULT PLANE DIPS

Catalogues of dip-slip earthquake focal mechanisms have previously been studied by Jackson & White (1989), Thatcher & Hill (1991), Sibson & Xie (1998), and Collettini & Sibson (2001). Sibson & Xie (1998) and Collettini & Sibson (2001) interpreted their results to represent faults with coefficients of friction ≥0.6 initiating at optimum angles of ∼60° (normal faults) or ∼30° (reverse faults), and rotating by ∼30° during displacement accumulation before experiencing frictional lock-up. Thatcher & Hill (1991) put forward a similar interpretation, and also an alternative in which dip angles are controlled by the ductile behaviour of the lower crust. Fault dip information can be related to the mechanics of faults because the angles at which fault planes can be active depend upon the frictional properties of the faults involved (e.g. Sibson 1985).

2.1 The use of low-displacement faults

In this paper, we take a different approach to the previous studies. Rather than using all available dip-slip focal mechanisms, many

*Now at: COMET+, Department of Earth Sciences, University of Oxford, Oxford, UK.

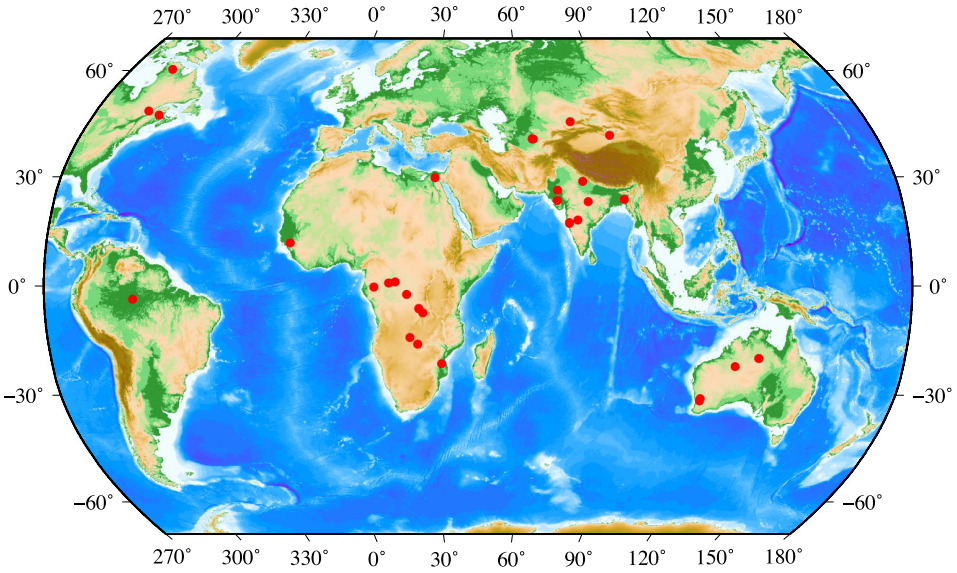

Figure 1. Locations of earthquakes used in this study. Note that some events occurred close together, so appear as one circle on a map of this scale.

of which are from areas where young, dipping sediments indicate significant rotation about horizontal axes (e.g. the Aegean; Jackson & White 1989), we restrict our catalogue and only use events from faults that show evidence of low total displacements (e.g. less than a few kilometres) during their current phase of activity (i.e. since initiation or reactivation). These faults are not known to be associated with significantly tilted recent deposits. Based on the observation that active faults often reactivate older structures (e.g. Berberian 1979; Allen & Vincent 1997; Hand & Sandiford 1999; Talebian *et al.* 2006), and that the continental crust is observed to be highly heterogeneous, we assume in this paper that the earthquakes we study have occurred on active faults that have reactivated older structures. We do not know for certain that all the events in our data set occurred on reactivated structures, but we note that our results are not dependent upon this assumption, as will be discussed when we return to the issue later.

The low-displacement nature of the faults we have selected means that they will not have undergone significant recent horizontal-axis rotation. Some of these faults may have accumulated large displacements during previous phases of activity, but the important aspect for our study is that they have not slipped by large amounts (e.g. more than a few kilometres) since reactivation. This means that the observed dips can be used to constrain the frictional properties of the faults at the onset of the current phase of motion. The exclusion of faults that have undergone considerable rotation removes an ambiguity in the interpretation of the fault dip data, where patterns could be due to either the angles of fault initiation, fault rotation, or both. In our study, if our assumptions are correct, the dip values should only depend upon the frictional properties of the faults. Additionally, the low-displacement nature of the faults we study means that the gravitational potential energy and flexure-related forces that accumulate with continued slip will be relatively minor.

The low-displacement faults are identified on the basis of having no geomorphological expression, other than fault scarps up to tens of metres high, which could have formed within a relatively small number of earthquakes. The geomorphology in the epicentral regions was examined using satellite-derived topographic data, and high-resolution optical imagery. We exclude aftershocks, but include events that are part of sequences of similar-sized earthquakes. The 36 events we have identified largely lie within slowly deforming regions, away from mountain ranges and rift valleys. The distribution of our chosen earthquakes is shown in Fig. 1, and the earthquake parameters are given in Table 1. Although subtle geomorphology can be obscured by erosion, our assumption that the faults are unlikely to have slipped by more than a few kilometres is based upon the fact that such slip would produce over a kilometre of relief at the surface, which even in the presence of rapid erosion would be likely to leave some visible remnant in the remote sensing and topographic data. Although this assumed upper bound on the fault slip may seem arbitrary, it is based on an extreme value of fault slip that we believe we would allow us to identify the presence of active faulting with significant total displacements. We expect many of the faults we have identified to have slipped by much lower amounts. We discuss below the implications of this assumption being wrong.

It is likely that the low-displacement faults we have identified currently dip at angles close to those at which they formed or were reactivated. For example, for a normal fault dipping at 45° in a set of rotating faults with 10–40 km spacings to rotate by 10° (similar to the possible uncertainties in the earthquake nodal plane dip determinations), it would have to generate more than 3–12 km of displacement (e.g. Jackson & McKenzie 1983, and as observed in regions such as the Aegean and Basin and Range). Similar results hold for reverse faults. We are likely to observe a significant geomorphological expression at an active fault that has accumulated such large amounts of slip, and so our methodology excludes those faults from our data set. We have included two earthquakes in our study which lie beneath the Ganges foreland basin (adjacent to the Himalaya and the Indo-Burman ranges). Although the thick piles of sediment would make it difficult to see geomorphology associated with these events, their presence in the relatively undeforming Indian crust suggests that their total recent fault displacements are likely to be low.

The remote and undocumented nature of many of the faults that broke in the earthquakes in our catalogue make testing the assumptions of reactivation, and low displacements during the present phase of tectonic activity, difficult. Additionally, in some cases observations of surface geology cannot easily assess the extent to which an earthquake may have reactivated older structures at depth.

Table 1. Parameters of earthquakes used in this study. References marked with a star used waveform modelling to estimate the source parameters, those without used *P*-wave first motion polarities.

Year	Month	Day	Lat	Lon	Mag	Strike	Dip	Rake	Reference
1966	8	15	28.67	78.84	5.6	132	31	−90	Molnar *et al.* (1977)
1967	12	12	17.22	73.78	5.7	100	40	−120	Langston & Franco-Spera (1985)
1968	5	15	−15.92	26.1	5.61	36	34	−113	*Foster & Jackson (1998)
1968	10	14	−31.52	116.98	6.64	351	29	73	*Fredrich *et al.* (1988)
1968	12	2	−14.11	23.78	5.6	35	36	−81	*Foster & Jackson (1998)
1970	3	24	−22.06	126.67	6.01	161	45	80	*Fredrich *et al.* (1988)
1971	2	2	23.72	91.64	5.4	119	36	90	Chen & Molnar (1990)
1974	9	23	−0.3	12.76	6.03	344	41	86	*Foster & Jackson (1998)
1976	4	8	40.36	63.73	6.81	91	43	80	*Kristy *et al.* (1980)
1976	5	17	40.4	63.42	6.85	25	56	78	*Kristy *et al.* (1980)
1979	6	2	−30.82	117.11	6.08	171	34	98	*Fredrich *et al.* (1988)
1979	9	25	45.09	76.96	5.4	77	44	119	*Nelson *et al.* (1987)
1981	11	18	−2.26	22.9	5.7	137	60	−44	*Craig *et al.* (2011)
1982	1	9	46.98	−66.66	5.6	170	50	90	*Hartzell *et al.* (1994)
1983	7	7	−7.35	27.94	5.83	224	42	−89	*Foster & Jackson (1998)
1983	8	5	−3.59	−62.17	5.5	305	60	120	Assumpcao & Suarez (1988)
1983	12	22	11.86	−13.51	6.27	112	48	−110	*Foster & Jackson (1998)
1984	3	19	40.36	63.32	6.86	210	40	83	*Eyidogan *et al.* (1985)
1987	12	12	41.32	89.66	5.3	195	50	115	*Bayasgalan *et al.* (2005)
1988	1	22	−19.88	133.83	6.47	117	30	100	*McCaffrey (1989)
1988	1	22	−19.9	133.85	6.63	102	38	82	*McCaffrey (1989)
1988	1	22	−19.87	133.8	6.34	269	52	63	*McCaffrey (1989)
1988	11	25	48.12	−71.18	5.9	320	65	78	*Hartzell *et al.* (1994)
1989	12	25	60.12	−73.6	5.9	50	42	90	*Hartzell *et al.* (1994)
1991	11	8	26.28	70.58	5.4	74	33	61	*Jackson (2002)
1992	9	11	−6.15	26.66	6.27	204	47	−119	*Foster & Jackson (1998)
1992	10	12	29.72	31.15	5.75	128	43	−69	*Foster & Jackson (1998)
1993	9	29	18.07	76.49	6.1	112	42	90	*Gupta *et al.* (1998)
1995	9	22	1.09	19.36	5.33	327	29	82	*Craig *et al.* (2011)
1995	12	11	−6.23	26.72	5.42	227	45	−74	*Craig *et al.* (2011)
1997	5	21	23.1	80.12	5.7	65	64	75	*Maggi *et al.* (2000)
1998	3	5	0.8	17.4	5.17	145	46	79	*Craig *et al.* (2011)
1998	4	26	0.86	17.34	5.32	341	54	80	*Craig *et al.* (2011)
2000	9	5	17.37	73.84	5.2	351	39	−94	*Priestley *et al.* (2008)
2001	1	26	23.42	70.23	7.5	82	51	77	*Antolik & Dreger (2003)
2006	2	22	−21.3	33.61	6.93	160	72	−71	*Craig *et al.* (2011)

However, for some of the earthquakes our assumptions can be tested. The 1993 Killari earthquake occurred in a region of India covered by Late Cretaceous–Eocene Deccan basalt flows. The lack of significant tilting of these basalts (Seeber *et al.* 1996) implies that displacements during the current phase of tectonic activity within peninsular India [which is likely to have begun coincident with the India–Asia collision, at a similar time to the basalt emplacement (e.g. Copley *et al.* 2010)] have been minor. The 2001 Bhuj (NW India) earthquake occurred in the region of a failed Mesozoic rift (e.g. Talwani & Gangopadhyay 2001), implying reactivation of a pre-existing structure. Adams & Basham (1989) suggested that the three thrust-faulting earthquakes in our catalogue in NE Canada (Ungava, Saguenay and New Brunswick) occurred on reactivated Palaeozoic and Mesozoic normal faults. Adams *et al.* (1992) conducted a detailed field investigation of one of these events (the 1989 Ungava earthquake) and concluded that at shallow depths the earthquake reactivated compositional layering and foliation in the Precambrian bedrock, but observed no visible evidence for previous Phanerozoic earthquakes on the fault. Although this observation does not necessarily rule out reactivation of pre-existing faults at depth, as suggested by Adams & Basham (1989), it does imply low amounts of recent displacement. The intraplate earthquakes in Australia studied by Crone *et al.* (1997) are thought to have reactivated older (often Precambrian) faults, although the total motion during their current phase of activity is not known. Palaeoseismic trenching across the scarps from the 1988 Tennant Creek (Australia) earthquakes revealed a single Quaternary event on one of the fault segments and no evidence of prehistoric earthquakes on the other two segments (Bowman 1992). The 1992 Cairo earthquake was studied by Badawy & Monus (1995), who conclude that it was likely to have reactivated a deep-seated fault. Similarly, Foster & Jackson (1998) believe it is probable that both of the 1968 earthquakes in western Zambia each reactivated part of the Mwembeshi Shear Zone fabric. Langer *et al.* (1987) report that the 1983 Guinea earthquake occurred in near-horizontal Ordovician and Silurian sedimentary rocks. Both Langer *et al.* (1987) and Dorbath *et al.* (1984) suggest that the earthquake occurred on a pre-existing fault system, but the lack of any significant horizontal-axis rotations of the country rock indicate that the total displacement on this fault system during its current stage of activity is low.

These events represent only a well-studied subset of the earthquakes in our catalogue, but they are consistent with our assumptions described above. Therefore, in the absence of further information we will assume that the assumptions hold true for all events in the catalogue. We will discuss below the implications of our results if our assumptions are wrong.

2.2 Earthquake nodal plane dips

Our approach is made possible by the increasingly large numbers of well-determined earthquake focal mechanisms. We only use events for which body-waveform modelling has been used to determine well-constrained focal mechanisms, or mechanisms that have been obtained using first-motion polarities where there is a good enough distribution of measurements to adequately constrain the nodal plane dips (references are given in Table 1). The most well-constrained mechanisms have dip error estimates of 5–10°, whilst the least well-constrained events that have been included may be in error by up to ∼15°.

Most of the focal mechanisms we include in our catalogue (32 of the 36 events, marked by stars on Table 1) were produced by waveform modelling of teleseismically recorded *P* and *SH* waves at epicentral distances of 30°–90°, using records from long-period seismometers or broadband seismograms filtered to periods of 15–100 s, and assuming a point source. The use of this method means that earthquakes in regions with poor instrument coverage (e.g. central Africa) are not a problem because they are usually well recorded by numerous stations at teleseismic distances (for the case of the African events, in Europe, Asia and at ocean island stations). Two early studies using this technique (Nelson *et al.* 1987; Taymaz *et al.* 1991) performed extensive tests to assess the reliability of the estimated focal mechanism parameters, and showed that for the events they studied (dating back to the mid-1960s) the potential error in the dip estimates of the events studied was ∼5°. Subsequent studies have obtained similar or lower estimates (e.g. Bernard *et al.* 1997). An exception is a study of earthquakes between 1962 and 1986 in the Tibetan Plateau that produced a slightly higher average dip error estimate of 9° (Molnar & Lyon-Caen 1989), although some of those events did not have well-enough constrained mechanisms to have been included in our catalogue if they had occurred in relevant regions. The comparison of seismological and geodetic estimates of earthquake fault plane dips (e.g. Talebian *et al.* 2006; Elliott *et al.* 2010) show that the seismological estimates are commonly within ∼5° of the independently constrained geodetic estimates. For the specific case of the 2006 Mozambique earthquake included in our catalogue, the estimate of Craig *et al.* (2011) made using teleseismically recorded body waveforms was different by 3° from the joint inversion of geodetic and seismic data performed by Copley *et al.* (2012).

These error estimates do not include the potential errors resulting from incorrect choices of near-source elastic structure for the events, which could affect both seismic and geodetic estimates of fault geometry. The effects of unmodelled structures in the source regions are to some extent reduced by the simultaneous inversion of *P* and *SH* waves for all seismograms simultaneously (e.g. Fredrich *et al.* 1988). Nelson *et al.* (1987) showed that unmodelled velocity contrasts shallower than the earthquake source affected the estimated depth, but had little effect on the nodal plane geometry. By repeating the inversions of Craig *et al.* (2011) for the 2006 Mozambique earthquake, we have confirmed that changes in the source velocity structure by up to 20 per cent change the best-fitting depth and moment of the event, but have little effect (i.e. <3°) on the dip estimate of the nodal planes. As noted by Fredrich *et al.* (1988), such insensitivity to the source velocity structure stems from the simultaneous inversion of all stations, and the condition that the source is constrained to be double-couple.

The potential errors in dip estimations in focal mechanisms produced using *P*-wave first motion polarities are extremely sensitive to the distribution of data with respect to the nodal planes, and therefore no general statements about potential dip errors inherent in the technique can be made. However, the four first-motion mechanisms we have included in our catalogue have observations that tightly constrain the nodal plane dips. We therefore think that our assumed error of up to 15° in the nodal plane dip estimates made using waveform modelling and first motion polarities is conservative, and the actual errors are probably lower than this.

Fig. 2 shows the observed distributions of reverse and normal fault nodal plane dips. For the majority of the earthquakes (shown in grey) the actual fault plane is not known, and in these cases both

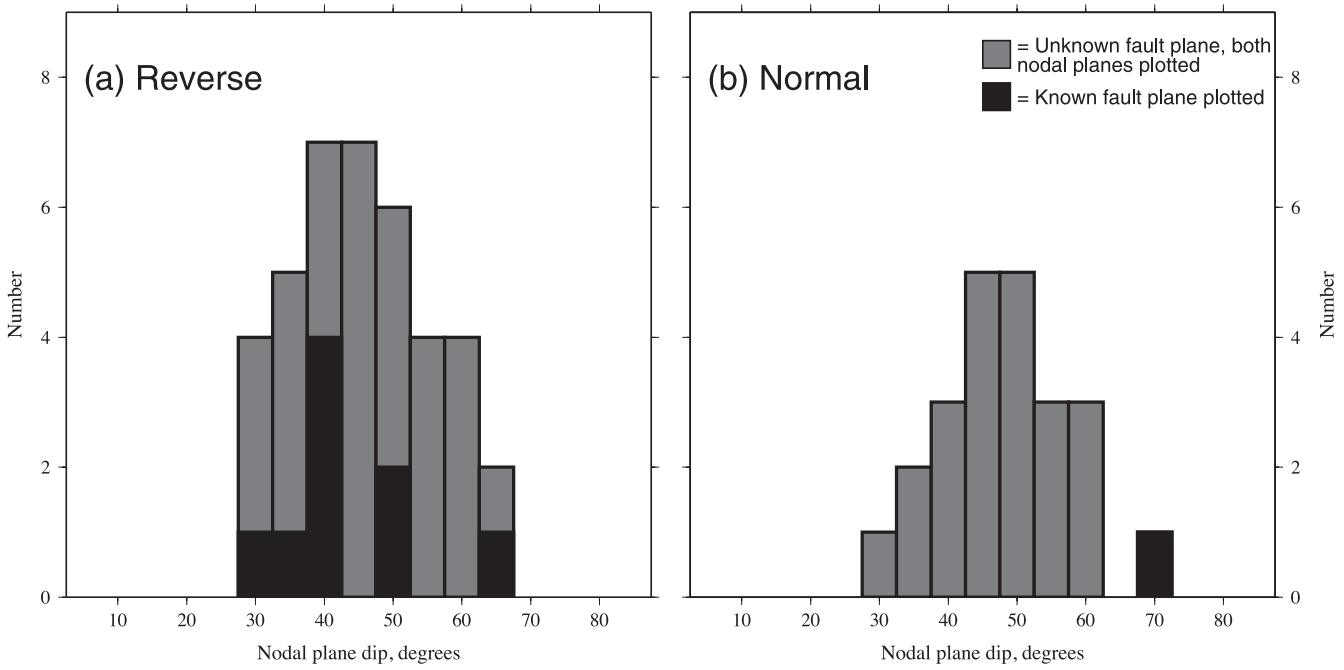

Figure 2. Reverse- and normal-faulting nodal plane dips. Black bars show known fault planes. Grey bars show both nodal plane dips for events where the fault plane is not known. Events with rakes within 45° of pure thrust or pure normal are included.

nodal planes are plotted. Both histograms show a lower limit to the nodal plane dips of ∼30°. Reverse fault nodal plane dips extend to ∼65°, and normal fault dips to ∼60°, with the addition of one known fault plane dipping at ∼70° (the 2006 Mozambique earthquake).

We first examine whether the observed distributions could be consistent with all faults dipping at either 30° (reverse faults) or 60° (normal faults), as predicted by 'Byerlee's Law'. In this case a single peak at 30° or 60° would be expected for events with known fault planes, and twin peaks at 30° and 60° for events where both nodal planes are plotted (given that most of the events are close to pure dip-slip). Because these values fall on the extremes of the observed distribution, even if we consider the errors associated with the nodal plane dip estimates, which are usually symmetrically distributed about the best-fitting estimate (e.g. Nelson *et al.* 1987; Molnar & Lyon-Caen 1989; Taymaz *et al.* 1991), this situation is incompatible with the distribution shown in Fig. 2. The pattern shown in Fig. 2 is remarkably similar to that observed by Jackson & White (1989) using all available normal-faulting focal mechanisms, and we will discuss this similarity in detail below. Thatcher & Hill (1991) described three possible situations that could give rise to the distributions of dip values observed by Jackson & White (1989), illustrated graphically in Fig. 3, which we can apply to our results: (1) all the fault planes could be clustered around 45°, or at dips within <10° of 45°, and the spread of values could represent errors in dip determinations; (2) there could be an equal distribution between 30° and 60°, and the addition of normally distributed errors could result in a distribution similar to that shown; (3) there could be a one-sided distribution, extending from 45° to either 30° or 60°, and the act of plotting both nodal planes and the addition of errors could result in a distribution similar to that observed. However, Thatcher & Hill (1991) also note that these latter two options would require dip estimation errors that are larger than suggested by the studies that obtained the focal mechanisms, and they favoured a single peak at close to 45° with a spread due to observational errors.

3 CONSTRAINTS ON FAULT FRICTION

Based on our earlier assumption that the earthquakes we have selected occurred on reactivated pre-existing structures, we will discuss the distribution of nodal plane dip values within the framework of the stresses required to reactivate faults of given dips, as put forward by Sibson (1985). We emphasize that because we think it likely that the faults we have studied are reactivating older structures, the coefficients of friction we estimate relate to mature fault zones, and not the initiation of new structures. Additionally, we make the assumption that on a global scale pre-existing heterogeneities are not limited to the dip range of the observed nodal planes. The widespread presence of low-angle thrusts and high angle strike-slip faults that could be reactivated, the horizontal-axis rotations that result from the mobility of the lower crust in some areas (e.g. McKenzie *et al.* 2000), and the presence of multiphase faulting in others (e.g. Proffett 1977), suggest that this assumption is justified.

By using the approach of Sibson (1985) to interpret the observed dip distribution we are making the commonly used assumption that the orientation of one principal stress is vertical (e.g. Thatcher & Hill 1991; Sibson & Xie 1998; Collettini & Sibson 2001). Under this condition, the ratio of principal stresses required to cause motion on a fault can be expressed as a function of the dip of that fault and its coefficient of friction. Estimating the coefficient of friction, for example by using the dips of fault planes as is done here, therefore cannot constrain the absolute magnitudes of the principal stresses (only the ratio of the minimum and maximum). If one of these values is known (e.g. by using the weight of the rock overburden to estimate the vertical stress) absolute values can be obtained.

Significant deviations from a state in which one of the principal stress orientations is vertical could result from large shear tractions on the base of the seismogenic layer or the lithosphere. None of the earthquakes in our catalogue are in crust that is itself being under- or overthrust by other material (those in forelands being sufficiently far from the zone of thrusting), or where large amounts of lateral flow in the lower crust are thought to be occurring, implying that any shear tractions on horizontal planes would only result from the shearing of the plates over the underlying mantle. Estimates of the tractions on the lithosphere–asthenosphere boundary are lower than the stress-drops commonly observed in earthquakes (e.g. Richter & McKenzie 1978; Copley *et al.* 2010), suggesting that the horizontal forces transmitted though the plates are larger than the tractions on the base, and that the deviation from the vertical of one of the principle stress axes is likely to be minor in the regions of the earthquakes in our catalogue. We therefore think it likely that the commonly used assumption of a vertical principal stress axis is justified, but note that our interpretations depend upon this assumption being correct.

Fig. 4(a) shows the ratio of principal stresses required to reactivate a fault of a given dip, calculated for a variety of coefficients of friction. Fig. 4(b) shows the dip of the minimum-differential-stress point on the reactivation curves shown in Fig. 4(a) (i.e. the dip at which faults can be reactivated with the minimum amount of tectonic forcing). If pre-existing structures are not present at all dips, faulting may occur anywhere within a range of angles rather than at the optimum orientation (Fig. 5a). This range extends to either side of the optimum dip, and faulting at anything other than the optimum angle requires higher differential stresses (Fig. 4a).

We will now consider the relationship between Fig. 4 and the three possible underlying fault populations that could generate the pattern observed in Fig. 2, as described above.

(1) If the fault planes are clustered at, or within <10° of, 45°, Fig. 4 suggests the reactivation of structures with a coefficient of friction less than ∼0.3 (with an unresolvable lower limit due to the possibility that the distribution could be single-valued and centred on 45°). It is for these values of the coefficient of friction that the reactivation curves are centred close to 45°.

(2) If the distribution spans ∼30° to ∼60°, it is symmetric about ∼45°, implying reactivation of structures with a low coefficient of friction (e.g. <0.1). It is only for these low coefficients of friction that the curves shown in Fig. 4(a) are symmetric about ∼45°.

(3) If the distribution of fault dips extends from 45° to either 30° or 60°, it must have a centre-point of either ∼37.5° or ∼52.5°, implying a coefficient of friction of less than ∼0.3. We view this possibility as least likely because our catalogue includes reverse faults with known fault planes that dip both steeper and shallower than 45°.

4 DISCUSSION

Based on the above arguments, we therefore suggest that the observed distribution of earthquake nodal plane dips implies the reactivation of structures with a coefficient of friction of less than ∼0.3. The spread in the range of observed dips could either represent inaccuracies in the determination of focal mechanisms, or the tectonic forces available in the regions we have studied (which will limit the distance away from the minimum points on the reactivation curves in Fig. 4(a) that faulting can occur). For simplicity,

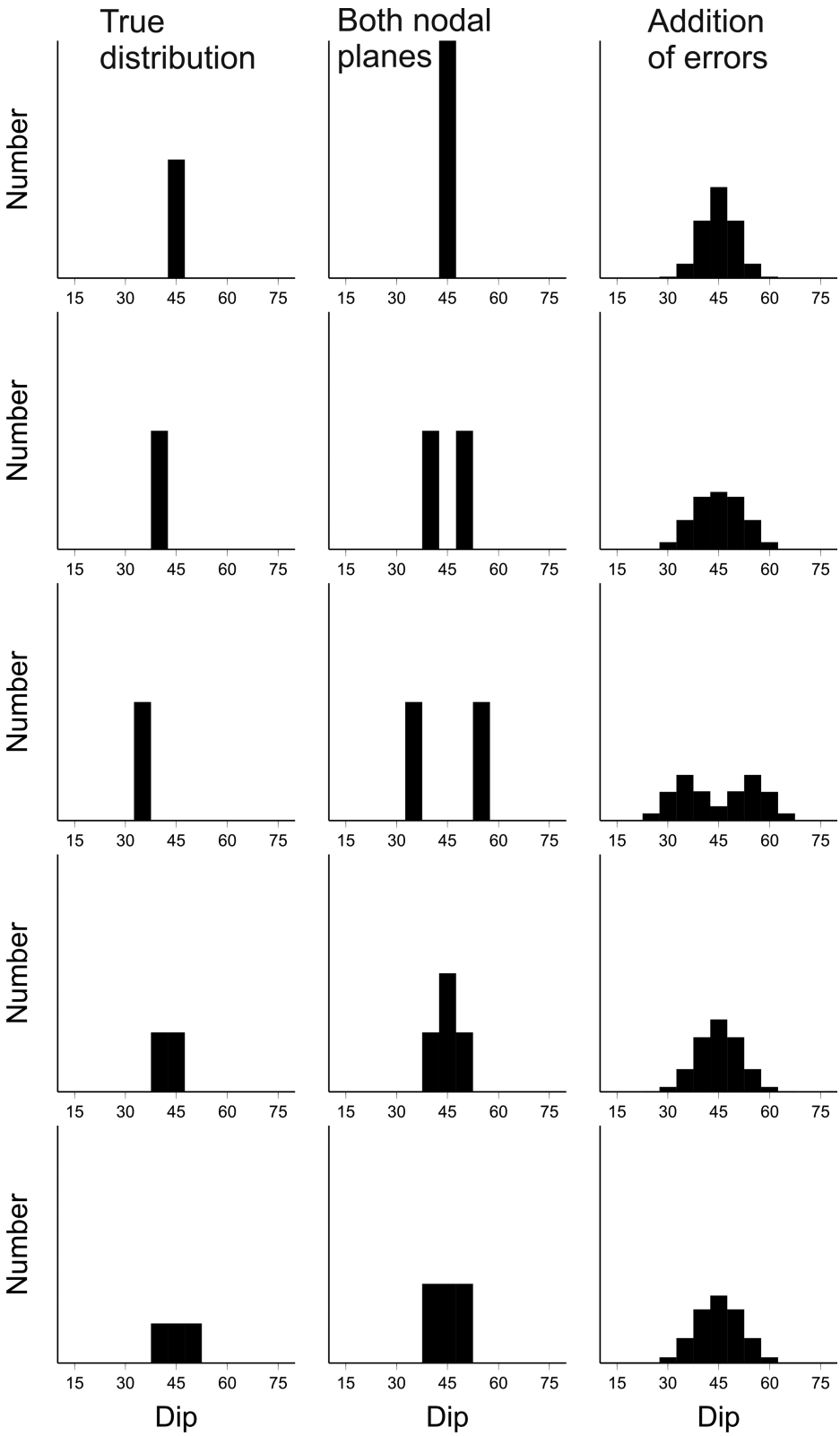

Figure 3. Adapted from Thatcher & Hill (1991). Synthetic histograms showing the relationship between a true distribution of fault planes, and the patterns observed if both nodal planes are plotted and normally distributed errors are added. Following Thatcher & Hill (1991) we calculated synthetic histograms using a normal distribution of errors, supported by the generally symmetrical dip error estimates obtained by waveform modelling studies (e.g. Molnar & Lyon-Caen 1989), implying no large skew is likely to be present in the distribution.

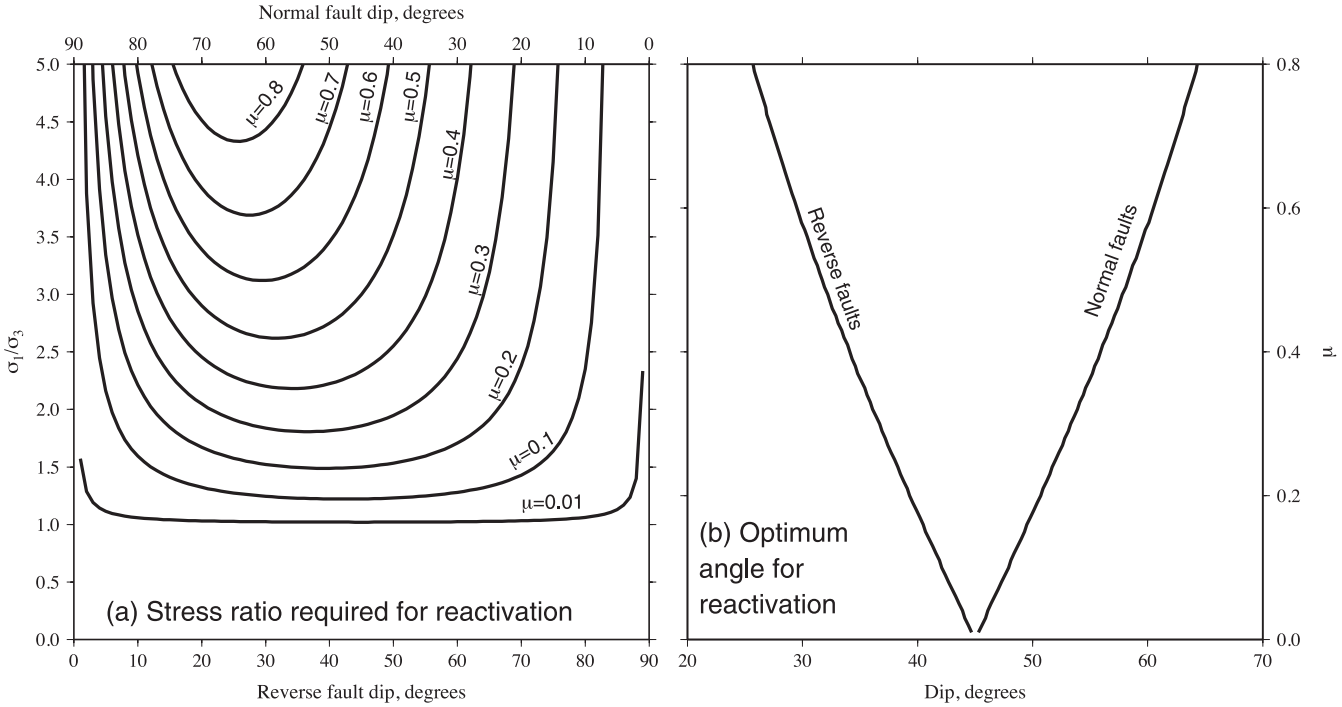

Figure 4. (a) The ratio of principal stresses required to reactivate faults of a given dip, as a function of the coefficient of friction [calculated using the expressions of Sibson (1985)]. σ_1 and σ_3 are the maximum and minimum principal stresses. (b) The optimum angle for reactivation of reverse and normal faults, as a function of the coefficient of friction.

in the preceding analysis we have assumed that the coefficient of friction is the same for all faults. There is a possibility that this is not the case, for example because of time-dependent fault-healing processes. Our estimated coefficient of friction corresponds to that on the faults in each region that could be most easily brought to failure. Such faults will slip in preference to faults with higher friction, or less optimal orientations. Arguments based upon the stress-drop of the 2001 Bhuj (NW India) earthquake suggest that faults in regions with strain rates too low to be measured at the continental scale by presently available geodetic techniques (e.g. <2 mm yr^{-1} over >1000 km; Bettinelli *et al.* 2006) can have low coefficients of friction (Copley *et al.* 2011), providing a limit on the degree of fault healing that can occur over even very long recurrence intervals.

4.1 Pore-fluid pressures and borehole observations

The effects of pore-fluid pressure on our results should be considered. If the coefficient of friction does not depend upon normal stress (and so the failure envelope plots as a straight line on Mohr diagrams), then increasing or decreasing the pore-fluid pressure will not change the optimum angle at which failure occurs (Fig. 5b). High pore-fluid pressures can reactivate non-optimally oriented structures, but only if no structures exist in an orientation closer to the optimum angle for failure. Assuming pre-existing heterogeneities exist at a wide range of angles, this situation would therefore imply that the observed earthquake dip distributions are insensitive to pore-fluid pressure, and that the low coefficients of friction we have suggested are due to inherently weak materials on the fault planes. It should also be noted that a variety of such weak materials have been observed to exhibit the velocity-weakening behaviour necessary for earthquake nucleation (e.g. Faulkner *et al.* 2010). If the coefficient of friction decreases with increasing normal stress (e.g. Byerlee 1978, Fig. 5c), then increasing the pore-fluid pressure would increase the optimum dip angles of normal faults (and decrease those of reverse faults). The observed distribution of fault plane dips would therefore imply low pore-fluid pressures and an inherently low coefficient of friction (with the value estimated above), or high pore-fluid pressures and an even lower coefficient of friction at larger effective normal stresses. We emphasize that we are not suggesting that pore-fluid pressures cannot be high, but that high pore-fluid pressures cannot be the root cause of our observations. We think it likely that some fault zones possess both low-friction materials along fault planes and also high pore-fluid pressures.

Two major patterns have emerged from borehole observations designed to investigate the mechanical properties of the crust. A suite of boreholes in a range of tectonic settings have suggested that the strength of the crust is controlled by faults with coefficients of friction of 0.6–1.0 and hydrostatic pore-fluid pressures (as summarized in Zoback & Townend 2001). In contrast, boreholes drilled through major active faults (e.g. Lockner *et al.* 2011), and the examination of rocks from exhumed fault zones (e.g. Collettini *et al.* 2009) have suggested low coefficients of friction (e.g. $\mu < 0.4$). These contrasting results are likely to be due to the differing methods used sampling different properties of the crust.

In situ borehole stress profiles are largely obtained through hydrofracturing and observations of borehole breakouts and drilling-induced fractures. These methods involve the creation of new fractures, or the reactivation of small, pre-existing features (less than tens of metres), which, because of the fault scaling relation between length and cumulative slip (e.g. Cowie & Scholz 1992) will have only experienced minor prior displacements. In contrast, experiments conducted on drill-core extracted from large faults (e.g. capable of rupturing in events of $M_w > 5.5$), or exhumed high-offset faults, are investigating the behaviour of structures that have accommodated considerably more displacement. Such results are consistent with a view that large fault displacements will produce fault gouge and weaken the fault zone as a whole.

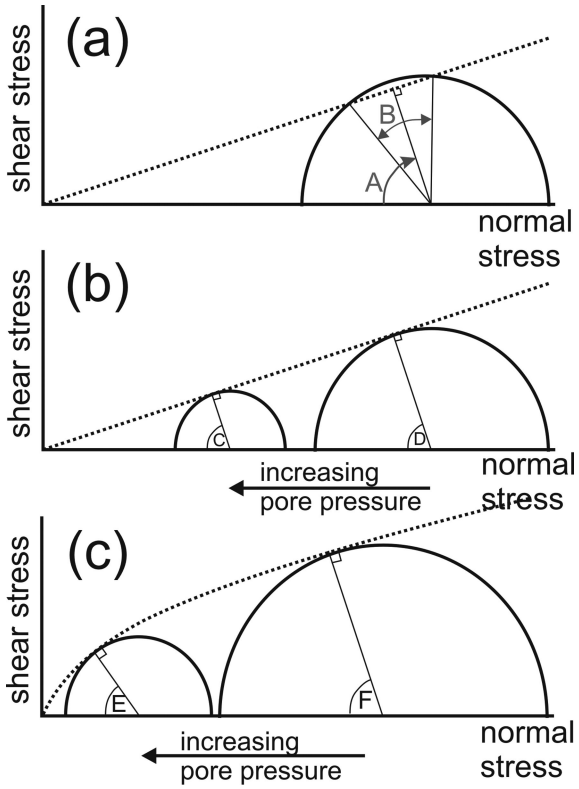

Figure 5. Mohr diagrams. (a) If pre-existing structures are not present at all angles, reactivation may occur over a range of dips (shown by B), rather than just at the optimum (shown by A, which represents twice the angle between the fault and the maximum principal stress direction). (b) If the coefficient of friction does not depend on normal stress, changing the pore-fluid pressure should not change the optimum angle for failure (i.e. C = D). (c) If the coefficient of friction decreases with increasing normal stress (e.g. Byerlee 1978), the optimum angle for failure moves closer to the principal stress direction as the pore-fluid pressure increases (i.e. E < F). Note that this result holds regardless of whether the failure envelope is a curve or two straight lines.

Our observations that imply low coefficients of friction for low-displacement faults may appear to contradict this pattern. However, this apparent disagreement stems from the definition of 'low displacement'. We think it likely that the faults we study have low total displacements for their current phase of activity, but that, because they are reactivating older structures, the fault planes themselves will have experienced considerable displacements over their lifetimes. Additionally, even if the faults we study have not reactivated older structures, the displacement-length scaling for faults (e.g. Cowie & Scholz 1992) implies that because we are looking at events of $M_w \geq 5$, the faults will have experienced orders-of-magnitude more displacement than the fractures on scales of centimetres to tens of metres formed or reactivated during borehole studies. Our results and the borehole observations are therefore consistent with a view in which large (kilometre-scale and above) low-friction faults are embedded in crust which is composed of high-friction rock which is unfaulted, or only contains minor and low-displacement fractures.

4.2 Comparison with global data sets, and exceptions to the general pattern

As noted above, our histogram of low-displacement fault dips is remarkably similar to those produced by Jackson & White (1989) and Collettini & Sibson (2001), who used all available dip measurements. Unless most faults are coincidentally at a similar point in their evolution from initiation, through rotation, to frictional lock-up, such a model can explain the endpoints of the distribution, but not the peak in the centre. Our results using our low-displacement fault database provide an alternative explanation. If many faults reactivate old structures, and these mature fault zones generally have low coefficients of friction, then reactivation would be expected at close to 45°. Depending on the geological histories of the regions experiencing active faulting, the faults may not be able to rotate far out of alignment before another pre-existing heterogeneity with a low coefficient of friction becomes rotated into alignment and fault activity switches onto that structure. Areas with diverse and complex geological histories, with many orientations of pre-existing fabric, may therefore be expected to show a concentration of fault dips at close to 45°. Furthermore, this logic implies that if our assumption of low fault displacements during the current phase of activity is wrong, then either our conclusion of low fault friction must remain unchanged, or there must be a global coincidence in the point in the initiation-rotation-lockup evolution reached by the dip-slip faults experiencing earthquakes.

The notable outlier in Fig. 2 is the steep dip of the 2006 Mozambique normal-faulting earthquake (the right-hand most point on the normal-faulting histogram). This event is situated on a low-displacement active fault at the southern tip of the East African Rift system (Copley *et al.* 2012). The anomalously high dip compared with the other events in the database could result from one of two situations. The first possibility is that the fault could have an extremely low coefficient of friction, which would allow faulting at a very wide range of dip angles (lowest curve on Fig. 4a). The other option is that the local stresses in this location could be higher than the other regions from which we have collated earthquakes (perhaps due to the position of the fault at the tip of the East African Rift). Higher differential stresses could result in failure over a greater range of dips for a given coefficient of friction (i.e. moving along a curve in Fig. 4a to higher stress ratios).

4.3 Formation of new fault zones

We now discuss our results in the context of the formation of new fault zones. If our suggestions above are correct, and low-friction materials lie along many fault planes, they are likely to be the result of cataclasis, fluid interactions, and mineralization within the fault zone following movement on the fault. We may therefore expect the coefficient of friction to be higher when faults first initiate in previously unfaulted country rock. The observed relatively steep dip at initiation of normal faults in the Yerington region of Nevada documented by Proffett (1977) may support this view.

If, as mentioned above, our assumption that the faults we are studying have reactivated older structures is in fact wrong, and we are observing slip on recently formed structures, then our conclusions nonetheless remain similar. New faults, which are not being guided by pre-existing structures, are expected to form at a common angle, determined by the coefficient of friction. The distribution of nodal plane dips in Fig. 2 suggests that if only one dip of faulting is observed, it must be close to 45°, and that the spread must represent errors in mechanism determination. An optimum dip angle at initiation of ~45° would imply a low coefficient of friction (≤0.1). However, based on the distribution of known reverse-faulting fault planes in Fig. 2, which span a larger range than would be expected to result from errors about one single central value, we view it as

more likely that the faults we have studied represent the reactivation of older structures.

5 CONCLUSIONS

We have studied the dip angles of earthquakes that occurred on low-displacement active dip-slip faults in the continents. The observed distribution suggests the reactivation of structures with coefficients of friction less than ∼0.3, and possibly as low as ≤0.1. We suggest that this coefficient of friction stems from the presence of weak materials along pre-existing fault zones.

ACKNOWLEDGEMENTS

Part of this work was undertaken when AC was supported by a research fellowship from Pembroke College in the University of Cambridge. We thank two anonymous reviewers for helpful comments on the manuscript. This work forms part of the NERC and ESRC funded project 'Earthquakes Without Frontiers'.

REFERENCES

Adams, J. & Basham, P.W., 1989. Seismicity and seismotectonics of Canada's eastern margin and craton, in *Earthquakes at North-Atlantic Passive Margins: Neotectonics and Postglacial Rebound, NATO ASI Series,* Vol. 266, Springer Netherlands, pp. 355–370.

Adams, J., Percival, J.A., Wetmiller, R.J., Drysdale, J.A. & Robertson, P.B., 1992. Geological controls on the 1989 Ungava surface rupture: a preliminary interpretation, *Current Research, Part C; Geological Survey of Canada, Paper 92-1C,* Geological Survey of Canada, pp. 147–155.

Allen, M.B. & Vincent, S.J., 1997. Fault reactivation in the Junggar region, northwest China: the role of basement structures during mesozoic-cenozoic compression, *J. geol. Soc. Lond,* **154,** 151–155.

Antolik, M. & Dreger, D.S., 2003. Rupture process of the 26 January 2001 Mw 7.6 Bhuj, India, earthquake from teleseismic broadband data, *Bull. seism. Soc. Am.,* **93,** 1235–1248.

Assumpcao, M. & Suarez, G., 1988. Source mechanisms of moderate-sized earthquake and stress orientation in mid-plate South America, *Geophys. J. Int.,* **92,** 253–267.

Badawy, A. & Monus, P., 1995. Dynamic source parameters of the 12th October 1992 earthquake, Cairo, Egypt, *J. Geodyn.,* **20,** 99–109.

Bayasgalan, A., Jackson, J. & McKenzie, D., 2005. Lithosphere rheology and active tectonics in mongolia: relations between earthquake source parameters, gravity, and GPS measurements, *Geophys. J. Int.,* **163,** 1151–1179.

Berberian, M., 1979. Earthquake faulting and bedding thrust associated with the Tabas-E-Golshan (Iran) earthquake of September 16, 1978, *Bull. seism. Soc. Am.,* **69,** 1861–1887.

Bernard, P. *et al.*, 1997. The ms=6.2, june 15, 1995 Aigion earthquake (Greece): evidence for low angle normal faulting in the Corinth rift, *J. Seismol.,* **1,** 131–150.

Bettinelli, P., Avouac, J-P., Flouzat, M., Jouanne, F., Bollinger, L., Willis, P. & Chitrakar, G.R., 2006. Plate motion of India and interseismic strain in the Nepal Himalaya from GPS and DORIS measurements, *J. Geod.,* **80,** 567–589.

Bowman, J.R., 1992. The 1988 Tennant Creek, Northern Territory, earthquakes: a synthesis, *Aust. J. Earth Sci.,* **39**(5), 651–669.

Brown, K.M., Kopf, A., Underwood, M.B. & Weinberger, J.L., 2003. Compositional and fluid pressure controls on the state of stress on the Nankai subduction thrust: a weak plate boundary, *Earth planet. Sci. Lett.,* **214,** 589–603.

Brudy, M., Zoback, M.D., Fuchs, K., Rummel, F. & Baumgartner, J., 1997. Estimation of the complete stress tensor to 8 km depth in the KTB scientific drill holes: implications for crustal strength, *J. geophys. Res.,* **102,** 18 453–18 475.

Byerlee, J., 1978. Friction of rocks, *Pure. Appl. Geophys.,* **116,** 615–626.

Chen, W.-P. & Molnar, P., 1990. Source parameters of earthquakes and intraplate deformation beneath the Shillong Plateau and the northern Indoburman ranges, *J. geophys. Res.,* **95,** 12 527–12 552.

Collettini, C., 2011. The mechanical paradox of low-angle normal faults: current understanding and open questions, *Tectonophysics,* **510,** 253–268.

Collettini, C. & Sibson, R.H., 2001. Normal faults, normal friction?, *Geology,* **29,** 927–930.

Collettini, C., Niemeijer, A., Viti, C. & Marone, C., 2009. Fault zone fabric and fault weakness, *Nature,* **462,** 907–911.

Copley, A., Avouac, J-P. & Royer, J-Y., 2010. The India-Asia collision and the Cenozoic slowdown of the Indian plate: implications for the forces driving plate motions, *J. geophys. Res.,* **115,** doi:10.1029/2009JB006634, 2010.

Copley, A., Avouac, J-P., Hollingsworth, J. & Leprince, S., 2011. The 2001 Mw 7.6 Bhuj earthquake, low fault priction, and the crustal support of plate driving forces in India, *J. geophys. Res.,* **116,** doi:10.1029/2010JB008137.

Copley, A., Hollingsworth, J. & Bergman, E., 2012. Constraints on fault and lithosphere rheology from the coseismic slip and postseismic afterslip of the 2006 Mw7.0 Mozambique earthquake, *J. geophys. Res.,* **117,** doi:10.1029/2011JB008580.

Cowie, P.A. & Scholz, C.H., 1992. Displacement-length scaling relationship for faults: data synthesis and discussion, *J. Struct. Geol.,* **14,** 1149–1156.

Craig, T.J., Jackson, J.A., Priestley, K. & McKenzie, D., 2011. Earthquake distribution patterns in Africa: their relationship to variations in lithospheric and geological structure, and their rheological implications, *Geophys. J. Int.,* **185,** 403–434.

Crone, A.J., Machette, M.N. & Bowman, J.R., 1997. Episodic nature of earthquake activity in stable continental regions revealed by palaeoseismicity studies of Australian and North American Quaternary faults, *Aust. J. Earth Sci.,* **44,** 203–214.

Dorbath, C., Dorbath, L., Gaulon, R., George, T., Mourgue, P., Ramdani, M., Robineau, B. & Tadili, B., 1984. Seismotectonics of the Guinean earthquake of December 22, 1983, *Geophys. Res. Lett.,* **11,** 971–974.

Elliott, J.R., Walters, R.J., England, P.C., Jackson, J.A., Li, Z. & Parsons, B., 2010. Extension on the tibetan plateau: recent normal faulting measured by INSAR and body wave seismology, *Geophys. J. Int.,* **183,** 503–535.

Eyidogan, H., Nabalek, J. & Tokoz, M.N., 1985. The Gazli, USSR, 19 March 1984 earthquake: the mechanism and tectonic implications, *Bull. seism. Soc. Am.,* **75,** 661–675.

Faulkner, D.R., Jackson, C.A.L., Lunn, R.J., Schlische, R.W., Shipton, Z.K., Wibberley, C.A.J. & Withjack, M.O., 2010. A review of recent developments concerning the structure, mechanics and fluid-flow properties of fault zones, *J. Struct. Geol.,* **32,** 1557–1575.

Foster, A.N. & Jackson, J.A., 1998. Source parameters of large african earthquakes: implications for crustal rheology and regional kinematics, *Geophys. J. Int.,* **134,** 422–448.

Fredrich, J., McCaffrey, R. & Denham, D., 1988. Source parameters of seven large Australian earthquakes determined by body waveform inversion, *Geophys. J. Int.,* **95,** 1–13.

Gupta, H.K., Rastogi, B.K., Mohan, I., Rao, C.V.R.K., Sarma, S.V.S. & Rao, R.U.M., 1998. An investigation into the latur earthquake of 1993 in southern india, *Tectonophysics,* **287,** 299–318.

Hand, M. & Sandiford, M., 1999. ntraplate deformation in central australia, the link between subsidence and fault reactivation, *Tectonophysics,* **305,** 121–140.

Hartzell, S., Langer, C. & Mendoza, C., 1994. Rupture histories of eastern north american earthquakes, *Bull. seism. Soc. Am.,* **84,** 1703–1724.

Herman, F. *et al.*, 2010. Exhumation, crustal deformation, and thermal structure of the Nepal Himalaya derived from the inversion of thermochronological and thermobarametric data and modeling of the topography, *J. geophys. Res.,* **115,** doi:10.1029/2008JB006126.

Jackson, J.A. & White, N.J., 1989. Normal faulting in the upper continental crust: observations from regions of active extension, *J. Struct. Geol.,* **11,** 15–36.

Jackson, J.A., 2002. Strength of the continental lithosphere: time to abandon the jelly sandwich? *GSA Today,* **12,** 4–10.

Jackson, J.A. & M^{c}Kenzie, D., 1983. The geometrical evolution of normal fault systems, *J. Struct. Geol.,* **5,** 471–482.

Kristy, M.J., Burdick, L.J. & Simpson, D.W., 1980. The focal mechanisms of the Gazli, USSR, earthquakes, *Bull. seism. Soc. Am.,* **70,** 1737–1750.

Lachenbruch, A.H. & Sass, J.H., 1980. Heat flow and energetics of the San Andreas Fault Zone, *J. geophys. Res.,* **85,** 6185–6222.

Lamb, S., 2006. Shear stresses on megathrusts: implications for mountain building behind subduction zones, *J. geophys. Res.,* **111,** doi:10.1029/2005JB003916.

Langer, C.J., Bonilla, M.G. & Bollinger, G.A., 1987. Aftershocks and surface faulting associated with the intraplate Guinea, west Africa, earthquake of 22 December 1983, *Bull. seism. Soc. Am.,* **77,** 1579–1601.

Langston, C.A. & Franco-Spera, M., 1985. Modeling of the Koyna, India, aftershock of 12 December 1967, *Bull. seism. Soc. Am.,* **75,** 651–660.

Lockner, D.A., Morrow, C., Moore, D. & Hickman, S., 2011. Low strength of deep San Andreas fault gouge from SAFOD core, *Nature,* **472,** 82–85.

Maggi, A., Jackson, J.A., Priestley, K. & Baker, C., 2000. A re-assessment of focal depth distributions in southern Iran, the Tien Shan and northern India: do earthquakes really occur in the continental mantle? *Geophys. J. Int.,* **143,** 629–661.

McCaffrey, R., 1989. Teleseismic investigation of the January 22, 1988 Tennant Creek, Australia, earthquakes, *Geophys. Res. Lett.,* **16,** 413–416.

McKenzie, D., Nimmo, F., Jackson, J., Gans, P.B. & Miller, E.L., 2000. Characteristics and consequences of flow in the lower crust, *J. geophys. Res.,* **105,** 11 029–11 046.

Molnar, P. & Lyon-Caen, H., 1989. Fault plane solutions of earthquakes and active tectonics of the Tibetan plateau and its margins, *Geophys. J. Int.,* **99,** 123–153.

Molnar, P., Chen, W.-P., Fitch, T.J., Tapponnier, P., Warsi, W.E.K. & Wu, F., 1977. Structure and tectonics of the Himalaya: a brief summary of relevant geophysical observations, in Colloque Internationaux du CNRS, No 268, Himalaya: Sciences de la Terre, Editions du Centre Nationale de la Reecherche Scientifique, Paris, pp. 269–294.

Nelson, M.R., McCaffrey, R. & Molnar, P., 1987. Source parameters for 11 earthquakes in the Tien Shan, central Asia, determined by P and SH waveform inversion, *J. geophys. Res.,* **92,** 12 629–12 648.

Priestley, K., Jackson, J. & McKenzie, D., 2008. Lithospheric structure and deep earthquakes beneath India, the Himalaya and southern Tibet, *Geophys. J. Int.,* **172,** 345–362.

Proffett, J.M. Jr, 1977. Cenozoic geology of the yerington district, nevada, and implications for the nature and origin of Basin and Range faulting, *Geol. Soc. Am. Bull.,* **88,** 247–266.

Richter, F. & McKenzie, D., 1978. Simple plate models of mantle convection, *J. Geophys.,* **44,** 441–471.

Saffer, D.M., Frye, K.M., Marone, C. & Mair, K., 2001. Laboratory results indicating complex and potentially unstable frictional behaviour of smectite clay, *Geophys. Res. Lett.,* **28,** 2297–2300.

Seeber, L., Ekstrom, G., Jain, S.K., Murty, C.V.R., Chandak, N. & Armbruster, J.G., 1996. The 1993 Killari earthquake in central India: a new fault in Mesozoic basalt flows?, *J. geophys. Res.,* **101,** 8543–8560.

Sibson, R.H., 1985. A note on fault reactivation, *J. Struct. Geol.,* **7,** 751–754.

Sibson, R.H. & Xie, G., 1998. Dip range for intracontinental reverse fault ruptures: truth not stranger than friction?, *Bull. seism. Soc. Am.,* **88,** 1014–1022.

Talebian, M. *et al.*, 2006. The Dahuiyeh (Zarand) earthquake of 2005 February 22 in central Iran: reactivation of an intramountain reverse fault, *Geophys. J. Int.,* **164,** 137–148.

Talwani, P. & Gangopadhyay, A., 2001. Tectonic framework of the Kachchh earthquake of January 26, 2001, *Seism. Res. Lett.,* **72,** 336–345.

Taymaz, T., Jackson, J. & McKenzie, D., 1991. Active tectonics of the north and central Aegean Sea, *Geophys. J. Int.,* **106,** 433–490.

Thatcher, W. & Hill, D.P., 1991. Fault orientations in extensional and conjugate strike-slip environments and their implications, *Geology,* **19,** 1116–1120.

Zoback, M.D. & Healy, J.H., 1992. In situ stress measurements to 3.5 km depth in the Cajon Pass Scientific Research Borehole: implications for the mechanics of crustal faulting, *J. geophys. Res.,* **97,** 5039–5057.

Zoback, M.D. & Townend, J., 2001. Implications of hydrostatic pore pressures amd high crustal strength for the deformation of intraplate lithosphere, *Tectonophysics,* **336,** 19–30.

Zoback, M.D. *et al.*, 1987. New evidence on the state of stress on the San Andreas fault system, *Science,* **238,** 1105–1111.